STUDY THE THERMAL AND ELECTRICAL PROPERTIES OF SOME MAGNESIUM-BORO-PHOSPHATE GLASSES CONTAINING VANADIUM OXIDE.

A. A. Bendary

Phys. Dept., Faculty of Science, Al-Azhar Univ., Nasr City, Cairo, Egypt.

ABSTRACT

Glasses having the molecular composition 20 M_gO - 30 B_2O_3 - (50-x) P_2O_5 – x V_2O_5 –- (x = 0, 5, 10, 15 and 20 mol %) have been prepared by the conventional melt quenching method. The thermal and electrical transport properties of the prepared glasses were thoroughly investigated by using differential thermal analysis technique and LCR meter-bridge with four fixed frequencies.

All the obtained thermal parameters are found to depend on the composition and heating rate. Both the activation energy of glass transition and activation energy of crystallization as well as the thermal stability are found to increase with the gradual increase of vanadium oxide content.

It was found that, all samples exhibit semi-conduction properties and the conduction mechanism was found to be the small polaron hoping at relatively low temperatures while at relatively higher temperatures, the correlated barrier hoping model was found to be dominant. Also, as vanadium oxide was gradually increased, the conductivity, dielectric constant and dielectric loss factor exhibit gradual increase.

Key words: Thermal properties of glass, Thermal stability; Glass; Glass transition temperature, Electrical conductivity, Dielectric properties.

e-mail address: dr_ayman_bendary@azhar.edu.eg

1. INTRODUCTION

Boro-phosphate glasses are highly durable when compared with pure borate or pure phosphate glasses [1, 2]. These glasses have found industrial appealing applications as solid electrolytes and glass solders…etc. They offer the possibility to change their structure and properties on changing their composition [3]. Kamitsos stated that such changes take place in either their anionic or cationic network elements or both of them [4]. Therefore, many researchers have extensively studied the chemical durability, physical, electric and dielectric properties of boro-phosphate glasses due to their applications in solid state batteries [5, 6].

The basic building units of these glasses are BO_4, PO_4 tetrahedra and BO_3 triangles, while oxygen anions have six sites, these are B–O–B, P–O–P, B–O–P, (bridging oxygen), P– O^-, B–O^-, (non-bridging oxygen) and P=O (terminal oxygen) [7 - 9]. Hadj Youssef [2] have stated that, in boro-phosphate glasses of high phosphate and low borate concentrations, the formation of B–O–P bridges causes the increase of the proportion of tetrahedral borate groups, while in boro-phosphate glasses of low phosphate and high borate concentrations, di-borate groups are gradually formed causing a rigid boro-phosphate glass network. The presence of BO_4 tetrahedral groups associated with B–O–P bands, induce a random ramification which rise the competence of boro-phosphate networks [9]. Also, the incorporation of BO_4 units into the chain like phosphate glasses act to convert the network from one dimensional to three dimensional networks due to the effect of boron cations that cross-link phosphate chains and layers. Such a cross linking increases the glass transition (T_g), glass crystallization (T_c) temperatures, glass density (ρ) and micro-hardness [8-10]. The formation of di-borate structure act to decrease the BO_4 units, hence all properties will be reversed expect for the micro-hardness [11-15].

It is known that, glasses are usually insulators, but phosphate glasses containing transition metal ions (TMIs) (such as vanadium), exhibit a semiconducting behavior. This is due to the hopping of small polaron

between different oxidation states of the TMI (from V^{4+} to V^{5+} ions). In this case, the small ionic ratio of (V^{4+}/V^{5+}) indicating n-type semiconductor properties [16]. Also, Alkali-rich glasses exhibit dominant ionic conduction [17,18] and considered as promising electrolytic glasses for the solid state batteries due to the fast ion conductors such as Li^+, Na^+, Ag^+, Mg^{2+},…. etc. [19]. Oxide glasses containing both alkali and TMIs show more variable electrical behavior. It results from anomalies in the conductivity of different orders of magnitude depending on the amount of alkali and TMI ions. The study of mixed electronic-ionic conductors is of valuable interest due to their various potential applications,as smart windows and cathodes in electrochemical cells [20, 21].

However this work aims to investigate the thermal and electrical properties of 20 MgO - 30 B_2O_3 - (50-x) P_2O_5 – x V_2O_5 –- (x = 0, 5, 10, 15 and 20 mol %) glasses. This study will cover a wide frequency range (from 0.12 kHz to 100 kHz) and a wide temperature range (from 300 to 575 K). The conduction mechanism that controls the electron hopping from low to high valence states of vanadium ions, will be also explored.

2. EXPERIMENTAL PROCEDURE

Glass samples having the general molecular formula 20 M_gO - 30 B_2O_3 - (50-x) P_2O_5 – x V_2O_5 –- (x = 0, 5, 10, 15 and 20 mol %) have been prepared by the melt quenching technique. The preparation was carried out by melting homogeneous mixtures of $NH_4H_2PO_4$, H_3BO_3, MgO and V_2O_5 (with purity not less than 99.5 %) in porcelain crucibles using an electric muffle furnace at 1200 $^\circ$C for 2 h. The melts were quenched between two pre-cooled copper plates to form (2cm x 2cm x 2mm) solid samples.

The experimental densities (ϱ_{exp}) of these glasses were measured by applying the liquid displacement method based on Archimedes principle, using toluene as an immersion liquid (of stable density ρ = 0.868 g/cm^3). Then the empirical density (ϱ_{emp}) values for the close

paced structure of the correspond compounds were also calculated. Both the experimental and empirical molar volume values were also calculated.

The calorimetric measurements are carried out by using (Shimadzu (50) (Japan)) differential thermal analyzer. The calorimeter was calibrated for each heating rate, using the well- known melting temperatures and melting enthalpies of zinc and indium supplied with the instrument. The values of the glass transition (T_g), extrapolated onset crystallization (T_c) and crystallization peak (T_p) temperatures, were determined within accuracy of ±2 K.

To obtain the electrical parameters of the studied samples, the obtained solid glasses were polished to get suitable shapes of constant area and thickness. For each sample, both sides will be coated with silver paste. All measurements have been carried out by using a computerized Stanford LCR bridge model SR 720 at four fixed frequencies [0.12, 1, 10, 100 kHz], and all measurements were performed over the temperature range from 300 to 575 K.

3. RESULTS AND DISCUSSION
3. 1. Density and Molar volume

Density of glass is a property of interest where it reflects any structural variations in a glass network, and the measured density of a glass is used usually to calculate many physical constants of such glass. It can be used also to confirm the amorphous nature by comparing the experimental and empirical results of both density and molar volume values of solid samples [22, 23]. The experimental density (ρ_{exp}) values were obtained by applying equation (1),

$$\rho_{exp} = \left[\frac{w_a}{w_a - w_t}\right]\rho_t \tag{1}$$

where w_a and w_t are the weights of a glass sample in air and toluene respectively and ρ_t is the density of toluene.

The empirical density (ρ_{emp}) values were also calculated by using equation (2),

$$\rho_{emp} = \sum_i^n w_i \rho_i \qquad (2)$$

where w_i is the fractional weight of an oxide in a glass sample and ρ_i is its density.

However, Fig. (1) shows the variation of both (ρ_{exp}) and (ρ_{emp}) as a function of V_2O_5 content. It appeared that, both ρ_{exp} and ρ_{emp} show approximately gradual linear increase with increasing V_2O_5 and the experimental densities are usually lower than those calculated empirically. The gradual increase of both densities may be due to the large difference between the molecular weights of both V_2O_5 and P_2O_5 [(181.88) and (141.94) g / mol, respectively].
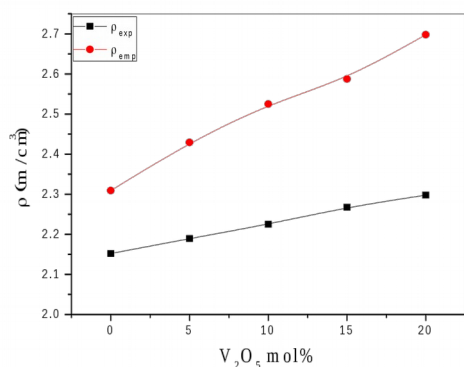

Fig. (1). The variation of the densities as a function of V_2O_5 content.

On the other hand, and for a good internal look inside the glass network, the molar volume can be considered, since it reflects directly the internal spatial structure of the material. Therefore, the experimental molar volume (V_m)$_{exp}$ was then calculated by using equation (3),

$$(V_m)_{exp} = M/\rho_{exp} \qquad (3)$$

where M is the mean molecular weight of a glass sample. The empirical molar volume (V_m)$_{emp}$ was also calculated by using equation (3) also, but with replacing ρ_{exp} by ρ_{emp}.

Fig. (2) shows the gradual change in both (V_m)$_{exp}$ and (V_m)$_{emp}$ values as V_2O_5 was gradually introduced, where a slight gradual linear increase can be observed, and the empirical values are usually lower than those measured experimentally [22].
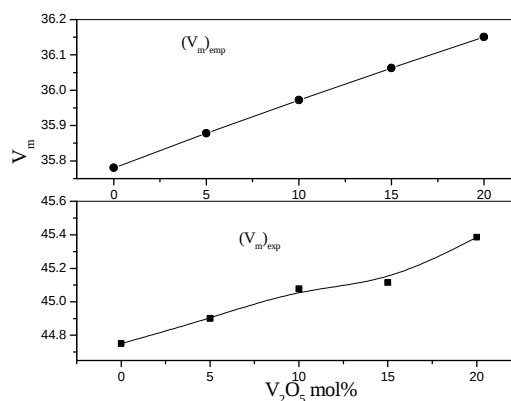

Fig. (2). The variation of the molar volume values as a function of V_2O_5 content.

It is supposed that, the gradual increase of both V_m values may be due to:

1- The replacement of smaller volume cations (the ionic radius of P = 0.38 Å) by a larger volume cation (the ionic radius of V = 0.59 Å).

2- The increase of the number of oxygen anions in the glass network, which can be calculated by using the following formula,

$$N = \sum \frac{X\% \, \rho \, N_A}{M} \qquad (4)$$

where X% is the mole percent of the dopant material, N_A is Avogadro number, and M is the average molecular weight [24, 25]. However, Fig. (3) shows that the number of oxygen ion concentration increased gradually and approximately linearly as V_2O_5 is increased.

From another point of view, it can be stated that, the higher empirical density values than those obtained experimentally and the lower empirical molar volume values than those obtained experimentally; can be taken as evidences for the amorphous nature and randomness character of the investigated samples [22, 23].
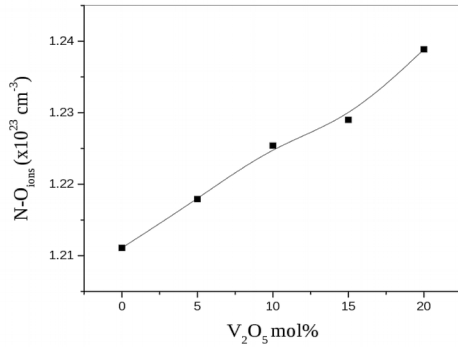
Fig. (3). The variation of the number oxygen ions density a function of V₂O₅ content.

3.2. Thermal analysis and thermal stability

Fig. (4) shows the DTA traces of the as-prepared samples at heating rate 10 K/min. All compositions exhibit single glass transition temperature followed by one crystallization peak. Fig. (5) shows the effect of varying the heating rate (β), on the thermal constants data for the glass sample containing 10 mol % V_2O_5 as represented curve (β = 5, 10, 15, 20 and 30 K/min). It is found that the thermal constants are shifted to higher temperatures with increasing the heating rate.
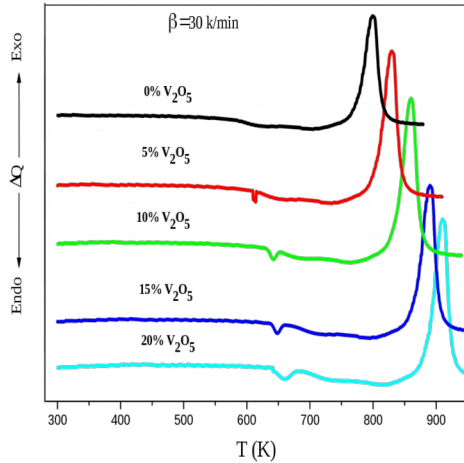

Fig. (4). Typical DTA traces for all glass samples at heating rate, β = 30 K/min.

The thermal stability criteria, $\Delta T = T_c - T_g$ [26], is a rough measure of the glass thermal stability, so the larger differences between T_c and T_g indicates more thermally stable glass, where T_c, is the onset temperature of crystallization. The thermal transition data T_g, T_c, and T_p and the thermal stability criteria, ΔT, at different heating rate (5, 10, 15, 20 and 30

K/min) are listed also in Table (1). The values of ΔT criterion of different compositions are listed in Table (1). With increasing V_2O_5 content, the thermal parameters (T_g, T_c and T_p) shifted to higher temperatures.

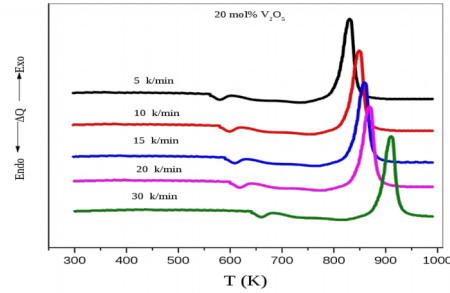parameters (T_g, T_c and T_p) shifted to higher temperatures.

Fig. (5). Typical DTA traces of the sample containing 10 mol % V_2O_5 at different heating rates, as represent figure.

Table (1). The values of the thermal parameters of all glasses at different heating states.

V_2O_5 (mol %)	β (K/min)	T_g	T_C	T_p	ΔT
0	5	510	721	800	211
	10	531	745	819	214
	15	562	778	834	216
	20	583	818	855	235
	30	615	869	895	254
5	5	525	741	809	216
	10	537	800	826	226
	15	567	810	851	243
	20	591	817	861	250
	30	610	870	889	257
10	5	560	780	831	220
	10	566	800	849	234
	15	576	815	860	239
	20	595	850	869	255
	30	610	875	910	265
15	5	572	798	839	226
	10	591	832	854	241
	15	594	842	868	248
	20	602	861	877	259
	30	619	885	920	266
20	5	581	810	845	229
	10	602	847	861	245
	15	607	857	880	250
	20	630	895	893	265
	30	648	918	940	270

The activation energy of enthalpy relaxation of the glass transition, or the activation energy of glass transition (E_g) of the

investigated glass, can be achieved by using Kissinger formula (equation. (5)), which is originally derived for the crystallization process and suggested to be valid for glass transition [27 - 30],

$$\ln\left(\frac{T_g^2}{\beta}\right) = \frac{E_g}{RT_g} + const \tag{5}$$

where R is the universal gas constant. The E_g values can be estimated from the $\ln(T_g^2/\beta)$ versus $1/T_g$ relation for different V_2O_5 contents. Fig. (6) shows the linear of relation of $\ln(T_g^2/\beta)$ versus $1000/T_g$ for the studied glasses.

The values of the glass transition activation energies (E_g) are evaluated also by the least squares fitting method of eq. (6), which is a simplified from of eqn. (5) [31], and the Fig. (7) the variation of the β versus $1000/T_g$ for all glasses.

$$\ln\beta = -\frac{E_g}{RT_g} + const. \tag{6}$$

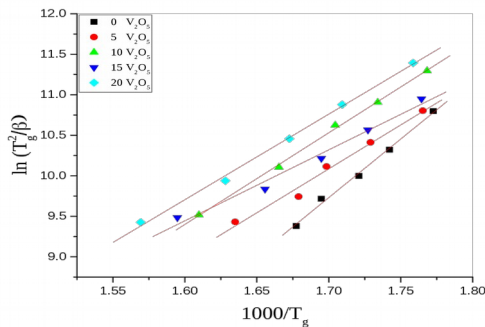It is found that the calculated activation energies by both equations (5 and 6) have nearly the same values.

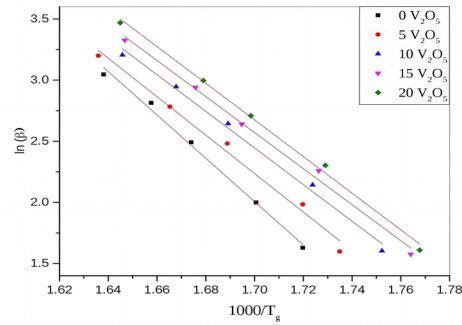**Fig. (6), ln (T_g^2/β) versus 1000/T_g for all glasses.**

Fig. (7), ln β versus 1000/T_g of all glasses.

The evaluation of the activation energy for crystallization (E_c) can be carried out by using the variation of crystallization peak temperature (T_p) with β applying equation (6) that developed the proposed method for non-isothermal analysis of devitrification [31].

$$\ln\left(\frac{T_p^2}{\beta}\right) = \frac{E_c}{RT_p} + \ln\frac{E}{RK_0} \tag{7}$$

Fig. (8) shows the relation of $\ln(T_p^2/\beta)$ versus $1000/T_p$ of all glasses. From the slopes of the obtained straight line fitting of the experimental data, the crystallization activation energy E_c, can be evaluated.
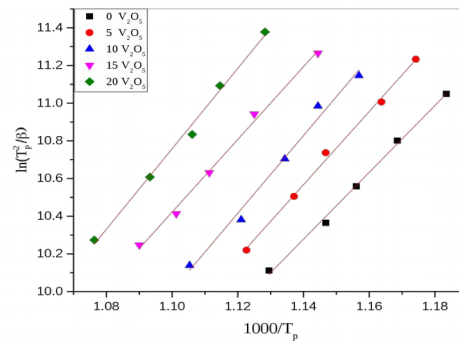

Fig. (8), ln(T_p^2/β) versus 1000/T_p of all glasses.

Fig. (9) (a) shows the variation of the glass transition activation energies (E_g) as a function of V_2O_5 content. It is found that, (E_g) increases with increasing V_2O_5 contents.

Fig. (9) (b) shows the variation of the crystallization activation energies (E_c) as a function of V_2O_5 content. It is found that the

crystallization activation energy increases with increasing V_2O_5 contents in the glass network.

Fig. (9) (c) shows the variation of the thermal stability criteria ($\Delta T = T_c - T_g$) [32, 34] as a function of V_2O_5 content. It is found that, ΔT increases with increasing V_2O_5 content, which means that, the partial replacement of P_2O_5 by V_2O_5 increases the glass stability of the studied glasses.
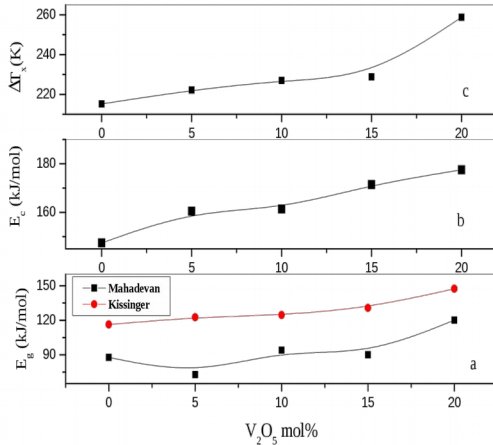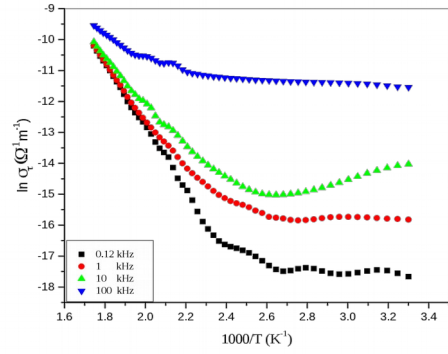

Fig. (10). The Variation of (σ_t) versus 1000/T for the sample containing 15 mol% V_2O_5, at different frequencies, as represented figure.

Therefore, by plotting $\ln\sigma_t(\omega)$ versus $\ln\omega$, at constant temperature, the exponent factor (s) can be calculated by using eq. (9),

$$S = \frac{\Delta ln(\sigma_t)}{\Delta ln(\omega)}$$

$$(9)$$

Fig. (11) represents the variation of the obtained values of s-factor with temperature where it shows firstly gradual increase up to 400 K, then it starts to decrease up to 550 K. Therefore, it can be stated that, between 300 and 400 K the small polaron hopping is the dominate conduction mechanism, while at temperatures higher then about 400 and up to 550, the correlated barrier hopping model is the dominate mechanism [36-40].
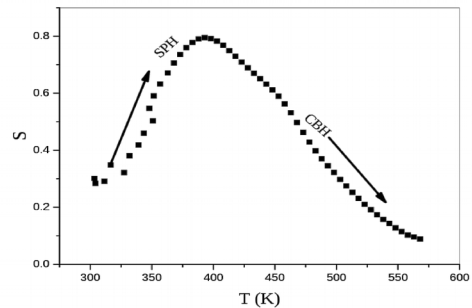

Fig. (9). The glass transition activation energy (E_g), the crystallization activation energy (E_c) and the thermal stability criteria (ΔT) as a function of V_2O_5 content.

3.3 ELECTRICAL CONDUCTIVITY

The temperature dependence ac conductivity at four frequencies (0.12, 1, 10 and 100 kHz) for the glass sample content 15 mol% V_2O_5 is exhibited in Fig. (10) as represented curve. The conductivity was found to increase with the increase of temperature, which reveals the semiconducting nature of the studied glass samples. It is known that, for all amorphous and glassy materials the measured conductivity during any experiment follows the relation [35, 36];

$\sigma_t(\omega) = \sigma_{dc} + \sigma_{ac} = \sigma_0 \exp(\Delta E_g/kT) + A\omega^s$ (8)

where A is a weakly temperature dependent factor, s is the exponent factor and ω is the angular frequency. At a constant temperature both σ_{ac} and $\sigma_t(\omega)$ have the same behavior but with different values.

Fig. (11). The variation of the exponent (s) with temperature for the sample containing 20 mol% V_2O_5, as represented figure.

For all the studied samples, it is clear that the conductivity $\sigma_t(\omega)$ increases with increasing temperature and such behavior refers to a thermally activated process between different localized states in the energy gap [41].

Also, it is clear that the conductivity $\sigma_t(\omega)$ shows weak frequency dependence at the high temperature range.

Fig. (12), shows the variation of the activation energy for conduction (ΔE) that obtained from the slopes of the fitted curves of $\sigma_t(\omega)$ (at high temperature) against 1000/T. it is appeared that ΔE decreased approximately linearly with increase of V_2O_5 content.

Fig.(13), exhibits the variation of $\sigma_t(\omega)$ as function of V_2O_5 content at different fixed temperatures. It can be seen that the conductivity increased with the increase of both temperature and V_2O_5 content, and this can be attributed to the increase of the thermally activated small polaron hopping (SPH) and the increase of electron hopping between (V^{3+}, V^{4+} and V^{5+}) [42]. Also, the increase in the free charge carriers in the network as a result to the increase of Mg^{2+} ions, due to the increase of molar volume (see Fig. 2) [43, 44].
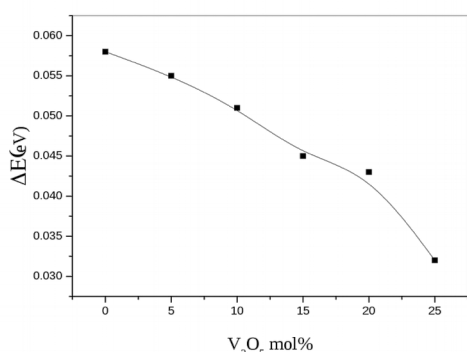

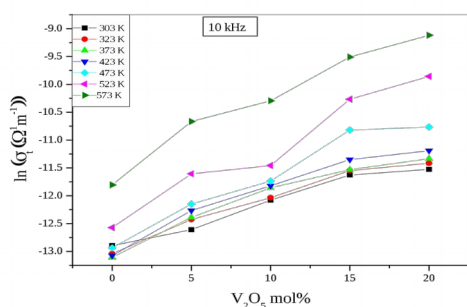**Fig. (12). The variation of the activation energy as a function of V_2O_5 contents.**

Fig. (13). The total conductivity as a function of V_2O_5 contents at different fixed temperatures.

3.4. Dielectric constant

The variation of the dielectric constant (ε') versus frequency and temperature for the sample contain 20 mol% V_2O_5 can be shown in Fig. (14), as a represent figure. It can be noticed that, ε' appeared to be stable up to certain temperature (T_o), difference from one sample to another. Then at such temperature, ε' starts to increase with temperature and inversely varies with the frequency, and similar behavior was observed for all samples. The obtained ε' values of the present glasses agree with the data reported by other authors [45, 46]. It is supposed that the increase of ε' with temperature is usually associated with the decrease in bond energies [46]. That is, as the temperature increases, two factors may affect the dipolar polarization,

(i) It weakens the intermolecular forces and hence enhances the orientational vibration.

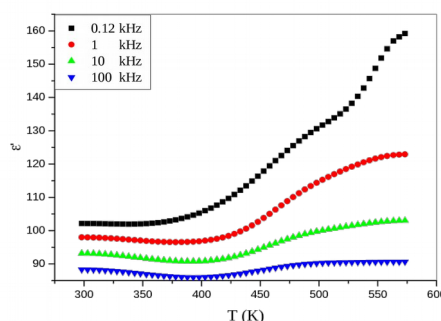(ii) It increases the thermal agitation and hence strongly disturbs the orientational vibrations.

Fig. (14). Frequency and temperature dependence dielectric constant for the sample containing 5 mol% V_2O_5, as represented figure.

The dielectric constant becomes larger at lower frequencies and at higher temperatures which is usually observed in oxide glasses and, is not an indication for spontaneous polarization [47]. This may be due to the fact that, as the frequency increased, the polarizability contribution from ionic and orientation sources decreased until complete disappearance due to the inertia of ions. This behavior is similar to the polar dielectrics in which the orientation of dipoles is facilitated

with rising temperature and thereby the dielectric constant increased.

At low temperatures, the contribution of electronic and ionic components to the total polarizability is small. As the temperature increased both the electronic and ionic polarizability start to increase. However, Fig. (15), exhibits the variation of ε' as a function of V_2O_5 content, at different fixed temperatures. From this figure it is evident that the dielectric constant increases with the increase of V_2O_5 concentration which can be attributed to the increase in the electronic contribution to the total polarizability [44, 48]. The compositional dependence of dielectric constant is very much similar to that of ac conductivity.
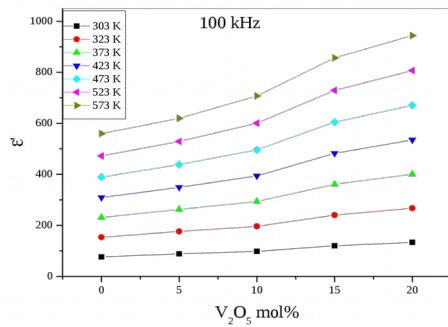

Fig. (15). The variation of the dielectric constant as a function of V_2O_5 contents at different fixed temperatures.

3.3. Dielectric loss

The frequency and the temperature dependence dielectric loss factor (ε'') for the studied glasses are shown in Fig. (16), where ε'' is found to increase with the increase of temperature and decrease with the increase of frequency. This may be due to the migration of ions, which is the major source of dielectric loss at low frequencies, while the higher values of ε'' at low and moderate frequencies can be attributed to the contribution arising from both ion jump and conduction loss in addition to the electron polarization loss. At higher frequencies the ion vibrations may be the only source of the dielectric loss [45, 46 & 49].
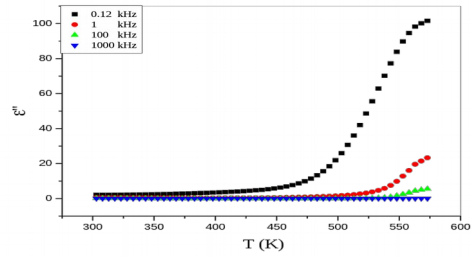

Fig. (16). Frequency and temperature dependence dielectric loss factor, for the sample containing 5 mol % V_2O_5, as represented figure.

The variation of ε'' suggests that the maximum loss could possibly occur at lower frequencies. From Fig. (16), it is noticed that ε'' increases with the increase of temperature. This can be attributed to the fact that, at low temperatures the relaxation loss is the main contributor and may be greater than the conduction loss. As the temperature increases, the relaxation loss decreases and hence the conduction loss increases more rapidly [44, 50].

Fig. (17), shows the compositional dependence of ε'' at 100 kHz and at different fixed temperatures, where ε'' is found to increase with the increase of V_2O_5 content. The compositional dependence of dielectric loss is also very similar to that of the ac conductivity and dielectric constant.
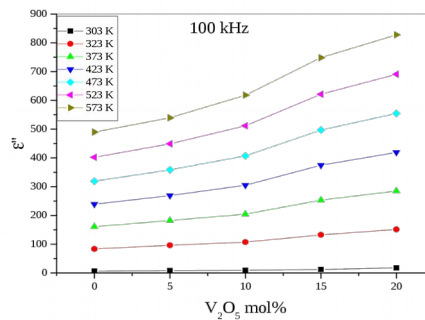

Fig. (17). The variation of the dielectric loss factor as a function of V_2O_5 contents at different fixed temperatures.

4. CONCLUSION

According to the above investigations and studies, the following conclusions can be drown,

1- All the prepared samples are found in good and homogenous amorphous glassy state as

drown from the comparison between both the experimental and empirical density and molar volume values.

2- The calculated thermal parameters (T_g, T_c and T_p) as well as the thermal stability (ΔT) increased with the increase of both vanadium oxide and heating rate.

3- The activation energy of glass transition (E_g) and the activation energy of crystallization (E_c) increased with the gradual increase of V_2O_5 content.

4- The thermal stability of the studied glasses is found to increase also with V_2O_5 content.

5- All the studied glasses exhibit semi-conduction properties and the conduction mechanism at relatively low temperatures is the small polaron hoping mechanism, while at relatively higher temperatures it is the correlated barrier hoping model.

6- Also, the gradual increase of V_2O_5 act to increase the electrical conductivity and to decrease the electrical activation energy.

7- Both the dielectric constant and the dielectric loss factor exhibit slight gradual increase with the gradual increase of V_2O_5 content.

REFERENCES

[1] K. Brahmachary, D. Rajesh, S. Babu and Y. C. Ratnakaram, J. Mol. Struct., 1064 (2014) 6.

[2] N. Hadj Youssef, M. S. Belkhiria, J. J. Videau and M. Ben Amara, J. Materials Letters, 44 (2000) 269.

[3] M. I. Abd El-Ati and A. A. Higazy, J. Mater. Sci., 35 (2000) 6175.

[4] E. I. Kamitsos, A. P. Patris, Karakassides and G. D. Chryssikos, J. Non-Cryst. Solids, 126 (1990) 52.

[5] J. W. Lim, M. L. Schmitt, R. K. Brow and S. W. Yung, J. Non-Cryst. Solids., 356 (2010) 1379.

[6] N. Kiran and A. Suresh Kumar, J. Mol. Struct., 1054 (2013) 6.

[7] D. Raskar, M.T. Rinke and H. Eckert, J. Chem. Phys. (C), 112 (2008) 12530.

[8] J. Jisak, L. Koudelka and J. Posisil, J. Mater. Sci., 42 (2007) 8592.

[9] K. Srinivasulu, I. Omkaram, H. Obeid, A. Suresh Kumar and J. L. Rao, J. Phys. Chem. (A), 116 (14) (2012) 3547.

[10] P. F. James and W. Shi, J. Mater. Sci., 28 (1993) 2260.

[11] N. Chanthimaa and J. Kaewkhaoa, Materials Today, 4 (2017) 6099.

[12] Xiaolin Wang, Qiuchun Sheng, Lili Hu and Junjie Zhang, J. Materials Letters, 66 (2012) 156.

[13] Randilynn Christensen, Jennifer Byer, Garrett Olson and Steve W. Martin, J. Non-Cryst. Solids, 358 (2012) 583.

[14] A. Langar, N. Sdiri, H. Elhouichet and M. Ferid, J. Alloys Compd., 590 (2014) 380.

[15] J. Kolár, T. Wágner, V. Zima, Š. Stehlík, B. Frumarová, L. Beneš, M. Vlcek, M. Frumar and S. O. Kasap, J. Non Cryst. Solids, 357 (2011) 2223.

[16] A. Langar, N. Sdiri, H. Elhouichet and M. Ferid, Eurpo. Phys. J. Plus, 131 (2016) 421.

[17] M. M. El-Deskoky and M.Y. Hassaan, Phys. Chem. Glasses, 43, 1 (2002). 2.

[18] A. Al-Hajry, N. Tashtoush and M. M. El-Desoky, Physica B, 368 (2005). 51.

[19] Andrea Moguˇs-Milankoviˊc, Kristina Sklepiˊc, Petr Moˇsner, Ladislav Koudelka and Petr Kalenda, J. Phys. Chem. (B), 120 (2016). 3978.

[20] K. M. Ereiba, A. S. Abd Raboh and A. G. Mostafa, Nat. Sci., 12, 5 (2014). 97.

[21] L. Murawski and R. J. Barczynski, Solid State Ionics, 176 (2005) 2145.

[22] A. M. Zoulfakar, A. M. Abdel-Ghany, T. Z. Abou-Elnasra, A. G. Mostafa, S. M. Salem and H. H. El-Bahnaswy, J. Applied Radiation and Isotopes, 127 (2017) 269.

[23] A. M. Abdel-Ghany, T. Z. Amer, A. A. Bendary and A. G. Mostafa, J. Nucl, & Part. Phys. 5, (2015) 101.

[24] G. Upender, S. Ramesh, M. Prasad, V.G. Sathe and V. C. Mouli, J. Alloy. Compd., 504 (2) (2010) 468.

[25] N. Elkhoshkhany, Ali Reda and Amira M. Embaby, J. Ceramics International, 43 (2017) 15635.

[26] M. Harish Bhat, Munia Ganguli and K.J. Rao, Curr. Sci., 86.5 (2004) 676.

[27] E. R. Shaabana, M. Y. Hassaan, A. G. Mostafa and A. M. Abdel-Ghany, J. Alloys and Compounds, 482 (2009) 440.

[28] Maria Lasocka, Mater. Sci. Eng., 23 (1976) 173.

[29] H. Yinnon and D. R. Uhlmann, J. Non-Cryst. Solids, 54 (1983) 253.

[30] E. Homer and Kissinger, Anal. Chem., 29 (1957) 1702.

[31] T. Ozawa, Chem. Soc. Jpn., 38 (1965) 1881.

[32] M. Shapaan, Int. J. New. Hor. Phys., **3 (**2) (2016) 55.

[33] R. El-Mallawany, A. Abdel-Kader, M. El-Hawary and N. El-Khoshkhany, J. Mater. Sci., 45 (2010) 871.

[34] S. A. Salehizadeh and D. Souri, J. Phys. Chem. Solids, 72 (2011) 1381.

[35] A. K. Jonscher, Nature, 267 (1977) 673.

[36] E. V. Gopalan, K. A. Malini, S. Saravanan, D. S. Kumar and Y. Yoshida, J. Phys. D Appl. Phys., 41 (2008) 185005.

[37] S. Seethalakshmi, B. Subramanian, Avi Bendavid and A. K. Nanda Kumar, J. Ceramics International, 43 (2017) 3202.

[38] N. F. MOTT, J. Non Cryst. Solids, 1 (1968) 1.

[39] M. H. Buraidah, L.P. Teo, S.R. Majid and A.K. Arof, Physica B, 404 (2009) 1373.

[40] S. R. Elliot, Philos. Mag., 36 (1977) 1291.

[41] A. S. Samsudin and M. I. N. Isa, Int. J. Polym. Mater., 61 (2012) 30.

[42] L. Murawski, C.H. Chung and J. D. Mackenzie, J. Non-cryst. Solids, 32 (1979) 91.

[43] H. Nefzi, F. Sediri, H. Hamzaoui and N. Gharbi, J. Solid State Chem., 190 (2012) 150.

[44] Moufida Saad, Wissal Stambouli, Nasr Sdiri and Habib Elhouichet, J. Materials Research Bulletin, 89 (2017) 224.

[45] A. Dutta, T. P. Sinha, P. Jena and S. Adak, J. Non-Cryst. Solids, 354 (2008) 3952.

[46] S. Jayaseelan, P. Muralidharan, M. Venkateswarlu and N. Satyanarayana, Mater. Chem. Phys., 87, (2–3) (2004) 370.

[47] G. Sahaya Baskaran, M. V. Ramana Reddy, D. Krishna Rao and N. Veeraiah, J. Solid State Communications, 145 (2008) 401.

[48] S. Vinoth Rathan and G. Govindaraj, Solid State Sci., 12, 730 (2010) 730.

[49] Zachary N. Wing and John W. Halloran, J. Ceramics International, 43 (2017) 4618.

[50] S. Chopra, S. Sharma, T. C. Goel and R.G. Mendiratta, Solid State Commun., 127 (4) (2003) 299.